Theoretical comparison between field-emission properties of carbon protrusions ranging from an isolated atom to multi-wall nanotubes

2003 J. Phys.: Condens. Matter 15 R177

(http://iopscience.iop.org/0953-8984/15/4/203)

INSTITUTE OF PHYSICS PUBLISHING JOURNAL OF PHYSICS: CONDENSED MATTER

J. Phys.: Condens. Matter **15** (2003) R177–R191 PII: S0953-8984(03)39783-8

TOPICAL REVIEW

Theoretical comparison between field-emission properties of carbon protrusions ranging from an isolated atom to multi-wall nanotubes

A Mayer[1,3], **N M Miskovsky**[2] **and P H Cutler**[2]

[1] Laboratoire de Physique du Solide, Facultés Universitaires Notre-Dame de la Paix, Rue de Bruxelles 61, B-5000 Namur, Belgium
[2] Departments of Physics, 104 Davey Laboratory, Penn State University, University Park, PA 16802, USA

E-mail: alexandre.mayer@fundp.ac.be

Received 18 July 2002, in final form 28 November 2002
Published 20 January 2003
Online at stacks.iop.org/JPhysCM/15/R177

Abstract

We present a review of field-emission properties of carbon protrusions standing on a metallic substrate. The transfer-matrix technique used for the scattering calculations takes account of three-dimensional aspects of the potential energy. The structures considered consist of a single carbon atom, half of a C_{60} molecule on a flat metallic substrate or on top of a metallic cylinder, open and closed (5, 5) nanotubes and the (5, 5)@(10, 10)@(15, 15) multi-wall structure. The results indicate that enhanced emission is obtained from the protrusions having the largest aspect ratio, (quasi-)localized states or allowing for the highest field penetration (due to an open rather than closed configuration, a reduced polarizability or because of adsorbed/bonded species). From the comparison between the total-energy distributions, it is found that the half C_{60} molecule has a (quasi-)localized state, which gives rise to a resonance in the emission (also when present at the apex of the closed (5, 5) nanotube). The results show that the field enhancement factor, as derived from a Fowler–Nordheim analysis of our data, is only an indicator for the quality of the emitter and does not justify all differences in the rates of emission.

[3] Author to whom any correspondence should be addressed.

0953-8984/03/040177+15$30.00

Contents

1. Introduction

Carbon emitters show interesting field-emission properties such as low extraction fields (macroscopic values of the order of a few volts per micron) and high current densities. Besides diamond and thin-film emitters, carbon nanotubes are currently being actively investigated. In general, their current–voltage characteristics are found to follow a Fowler–Nordheim type tunnelling law [1–4] with an emitter work function around 5 eV depending on the type of nanotube.

The emission properties of carbon emitters are however still not clearly understood. Concepts of negative electron affinity, band bending and conducting channels are used to explain the emission from diamond and thin films [5–8], while the emission properties of carbon nanotubes are essentially attributed to their high field enhancement factor [9, 10], as deduced from the Fowler–Nordheim equation [11, 12]. For carbon nanotubes, it is known that electronic states localized near or at the apex of the structure influence the current emission profile [13, 14]. These localized states are relatively well documented for various kinds of tube termination [15–19] and can be induced by the extraction field [20].

The objective of this paper is to present a review of field-emission properties of various carbon emitters (ranging from an isolated atom to the (5, 5)@(10, 10)@(15, 15) multi-wall nanotube) and discuss various factors influencing the emission. Our results are obtained by solving numerically the Schrödinger equation with a three-dimensional potential-energy distribution representative of both the emitter's structure and the surface barrier. For the calculation of the potential energy, we used the techniques presented in [21] with the Bachelet *et al* [22] pseudopotentials for the representation of carbon atoms. The transfer-matrix methodology used for the scattering calculations has been described in previous publications [23, 24].

The organization of this paper is as follows. In section 2 we describe the main lines of our model. Section 3 then presents the results of field emission from a single carbon atom, half of a C_{60} molecule on a flat metallic substrate or on top of a metallic cylinder, closed and open (5, 5) nanotubes and a (5, 5)@(10, 10)@(15, 15) multi-wall structure. The differences in the emission rates are traced to the physical properties of the emitters considered. Section 4 is a discussion on the relevance of the field enhancement factor, as derived from a Fowler–Nordheim analysis of our data, to justify the differences between the emitters. We also point out some issues in the understanding of carbon emitters.

2. Theory

The emitter considered in each set of simulations stands on a flat metallic substrate (region I, $z \leqslant 0$). The extraction field results from an electric bias V, which is established between the metallic substrate in region I and the field-free vacuum (region III, $z \geqslant D$). The potential energy in the intermediate region II ($0 \leqslant z \leqslant D$) is calculated by using the techniques of [21], with a pseudopotential for the ion-core potential [22]. The electronic density associated with the four valence electrons of each carbon atom are represented by the sum of two Gaussian distributions (with parameters given in [22]). These electronic densities are displaced from the nuclear positions according to the polarization $\boldsymbol{p}_j$ of each atom. The dipoles $\boldsymbol{p}_j$ are calculated [23] by taking account of the extraction field, dipole–dipole interactions and the anisotropic polarizability [25] of the carbon atoms. The electronic exchange energy is evaluated by using the local density approximation $\frac{4}{3}C_X\rho^{1/3}$, where $\rho(\boldsymbol{r})$ is the local electronic density and $C_X = -3/4(e^2/4\pi\epsilon_0)(3/\pi)^{1/3}$ [21].

The electronic scattering from the metallic substrate (region I) to the vacuum (region III) is calculated by the transfer-matrix technique described in [23, 24]. In this formulation, the electrons involved in the transport remain localized inside a cylinder of radius R in the regions preceding the vacuum region III (R is chosen large enough so the results are independent of its particular value). Taking advantage of the cylindrical symmetry, the wavefunction is expanded in terms of basis states in region I as $\Psi^{I,\pm}_{m,j} = A_{m,j}J_m(k_{m,j}\rho)\exp(\mathrm{i}m\phi)\exp\left(\pm\mathrm{i}\sqrt{\frac{2m}{\hbar^2}(E - V_{\mathrm{met}})}z\right)$ and in the anode plane $z = D$ as $\Psi^{D,\pm}_{m,j} = A_{m,j}J_m(k_{m,j}\rho)\exp(\mathrm{i}m\phi)\exp\left(\pm\mathrm{i}\sqrt{\frac{2m}{\hbar^2}E}z\right)$, where the $A_{m,j}$ are normalization coefficients, J_m Bessel functions, $k_{m,j}$ transverse wavevector solutions of $J_m(k_{m,j}R) = 0$, E the electron energy and V_{met} is the potential energy in the supporting metal. The $\pm$ signs refer to the propagation direction relative to the z-axis, which is oriented from region I to region III. The transfer-matrix methodology [23] then provides scattering solutions of the form

$$\Psi^{+}_{m,j} \overset{z\leqq 0}{=} \Psi^{I,+}_{m,j} + \sum_{m',j'} t^{-+}_{(m',j',m,j)}\Psi^{I,-}_{m',j'} \overset{z\geqslant D}{=} \sum_{m',j'} t^{++}_{(m',j'),(m,j)}\Psi^{D,+}_{m',j'}, \tag{1}$$

corresponding to single incident states $\Psi^{I,+}_{m,j}$ with a unit amplitude (the transfer matrices t^{-+} and t^{++} contain the coefficients of the reflected and transmitted states). Total current densities result from the contribution of every solution associated with a propagative incident state in the supporting metal.

3. Application: review of field-emission properties of carbon protrusions

We investigated in previous publications [26–30] transport and field-emission properties of single-wall and multi-wall carbon nanotubes. Our methodology enables one to compute energy distributions with appropriate band-structure effects (bandgap of semiconducting tubes [27], constant density of states around the Fermi level of metallic ones [28] and van Hove singularities [18, 31]). For the small tube lengths considered, we could derive the existence of oscillations in the energy distributions, which are associated with stationary waves in the structure [27, 28]. Their number and sharpness were indeed found to increase with the length of the tubes. The existence of these oscillations, which actually come from the reflection of propagating states at the extremities of the nanotubes, has been observed experimentally [32]. These features were calculated for both biased and unbiased nanotubes.

Our study of field-emission properties of carbon nanotubes included those of the semiconducting (10, 0) [27, 30]. The existence of a gap in the energy distribution of the

semiconducting tubes [27, 33] makes them unsuited for applications as (non-stimulated) field emitters, since they compare badly with metallic nanotubes that have a non-zero density of states at the Fermi level (where the probability for electrons to escape to the vacuum is higher). The semiconducting nanotubes are however interesting for applications as photon-stimulated field emitters. Indeed it turns out that photon stimulation can increase, by orders of magnitude depending on the photon energy and the power-flux density of the radiation, the current emitted from semiconducting structures, thus providing an efficient way to control the rate of emission (by the radiation instead of the electric field) [30]. The current enhancements obtained by irradiating semiconducting tubes are several orders of magnitude higher than those obtained when irradiating metallic ones. The origin of this difference is the intrinsic emission (without stimulation) of semiconducting tubes being orders of magnitude lower than that of metallic ones. For a local field of 2.5 V nm^{-1}, a difference by eight orders of magnitude was found when comparing the current enhancement obtained with the semiconducting (10, 0) and the metallic (5, 5) nanotubes.

Only metallic structures will be considered in this paper. Our objective is to present a review of field-emission properties of carbon protrusions ranging from a single atom to a multi-wall (5, 5)@(10, 10)@(15, 15) nanotube. We examine the dependence of the emission rate on various parameters, including the length and polarizability of the protrusion. We also check the relevance of the Fowler–Nordheim equation [11, 12] to account for our data. For the modelling of the supporting metallic substrate, we use the same parameters as those chosen to reflect the properties of infinite nanotubes in [26, 28], i.e. an internal potential energy and a Fermi level respectively 16 and 5.25 eV lower than the vacuum level. The simulations assume local extraction fields V/D of 2, 2.5 and 3 V nm^{-1} (resulting from a fixed bias V of 12 V and cathode–anode distances D of 4, 4.8 and 6 nm). Finally the temperature T is 298 K.

3.1. Field emission from a single carbon atom

The first emitter considered consists of a single carbon atom (a similar situation is presented in [34]). We assume that it stands 0.071 nm above the flat metallic substrate, which is half the length of a C–C bond in the structures considered hereafter. The potential-energy distribution corresponding to an extraction field of 3 V nm^{-1} is illustrated in figure 1. The total-energy distributions of the field-emitted electrons, as obtained with applied electric fields of 2, 2.5 and 3 V nm^{-1}, are represented in figure 2.

The three distributions have the usual shape associated with a field-emission process. The current extracted for the three values of the electric field is respectively 0.19×10^{-21}, 0.11×10^{-17} and 0.36×10^{-15} A. When the corresponding I–V characteristic is represented in Fowler–Nordheim coordinates, a perfect alignment of our data is found and a field enhancement factor of 2.3 can be derived from the slope of the line.

3.2. Field emission from half of a C_{60} *molecule*

In the next simulations, we consider half of a C_{60} molecule on a flat metallic substrate (a similar situation with a hemispherical protrusion is presented in [35]). The first carbon atom is at a distance of 0.061 nm from the surface. This is the distance to a plane passing exactly through the middle of a complete C_{60} molecule (we assume that it stands on a pentagon). The potential-energy distribution corresponding to an extraction field of 3 V nm^{-1} is illustrated in figure 3. The total-energy distributions of the field-emitted electrons, as obtained with applied electric fields of 2, 2.5 and 3 V nm^{-1}, are represented in figure 4.

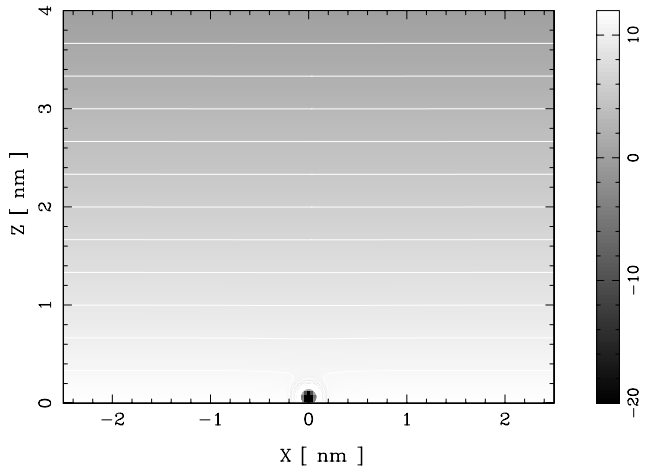

Figure 1. Potential-energy distribution (section in the xz-plane) corresponding to single carbon atom, a cathode–anode distance of 4 nm and a bias of 12 V.

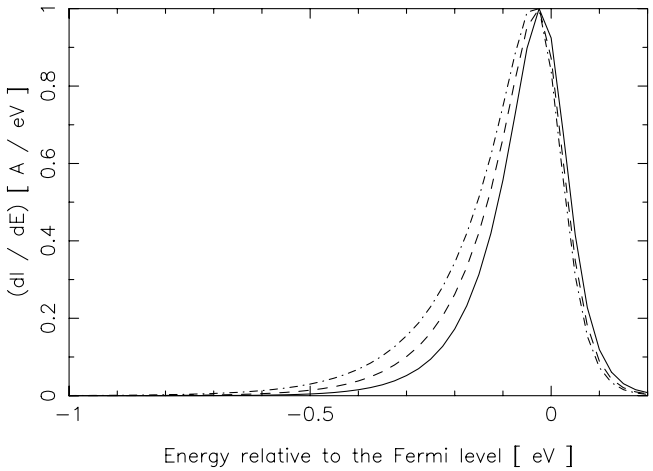

Figure 2. Total-energy distribution of electrons field-emitted from a single carbon atom, for applied electric fields of 2 (solid), 2.5 (dashed) and 3 (dot–dashed) V nm^{-1}. The maxima of the three distributions are respectively 0.104×10^{-20}, 0.522×10^{-17} and 0.159×10^{-14} A eV^{-1}.

The shape of the distributions is again that expected from a Fowler–Nordheim analysis of the field-emission process, with in addition a small bump (hardly visible) at 0.3 eV below the Fermi level for the 3 V nm^{-1} extraction field. This bump is related to a (quasi-)localized state in the half C_{60} molecule and appears more clearly when this structure stands on a metallic cylinder (see next subsection).

The current extracted for the three values of the electric field is respectively 0.51×10^{-21}, 0.37×10^{-17} and 0.17×10^{-14} A. On average, this is around three times the currents obtained with the single carbon atom. The Fowler–Nordheim representation of these data gives a straight line with a slope indicating a field enhancement factor of 2.2. This number is very close to the 2.3 value found for the single carbon atom, although the currents are higher (because of a deeper penetration in the potential barrier).

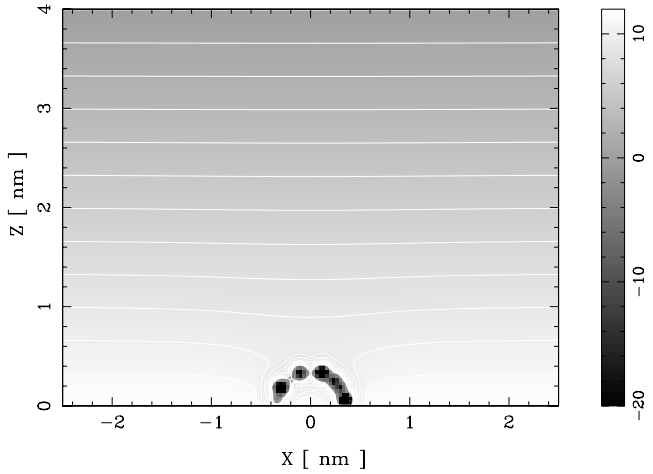

Figure 3. Potential-energy distribution (section in the xz-plane) corresponding to half of a C_{60} molecule, a cathode–anode distance of 4 nm and a bias of 12 V.

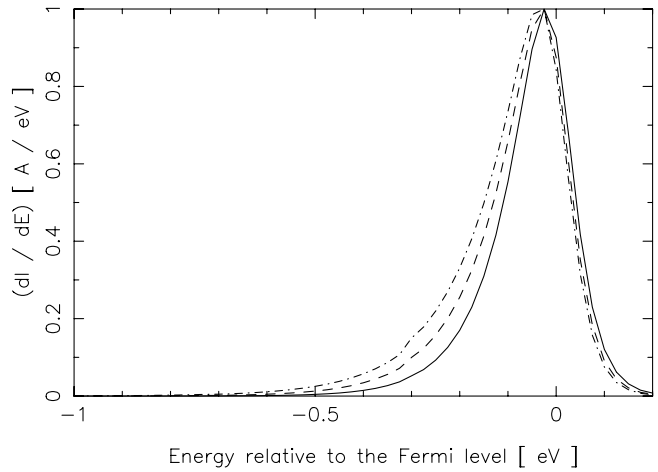

Figure 4. Total-energy distribution of electrons field-emitted from half of a C_{60} molecule, for applied electric fields of 2 (solid), 2.5 (dashed) and 3 (dot–dashed) V nm^{-1}. The maxima of the three distributions are respectively 0.283×10^{-20}, 0.183×10^{-16} and 0.765×10^{-14} A eV^{-1}.

3.3. Field emission from half of a C_{60} molecule on top of a metallic cylinder

In the next configuration, the half C_{60} molecule stands on top of a metallic cylinder. The radius and length of the cylinder are respectively 0.399 and 1.720 nm, so the half C_{60} molecule coincides with the cap of the closed (5, 5) nanotube considered hereafter and the distance from the half C_{60} to the cylinder is the same as that to the metallic substrate in the previous set of simulations. The radius and height of the cylinder are actually 0.06 nm larger than the body of the (5, 5) nanotube to guarantee these conditions and take account of the width of the atomic potentials. The potential-energy distribution corresponding to an extraction field of 3 V nm^{-1} is illustrated in figure 5. The total-energy distributions corresponding to applied electric fields of 2, 2.5 and 3 V nm^{-1} are illustrated in figure 6.

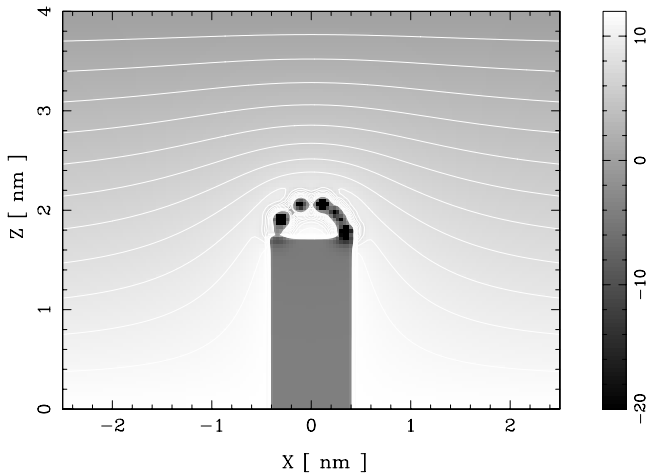

Figure 5. Potential-energy distribution (section in the xz-plane) corresponding to half of a C_{60} molecule on top of a metallic cylinder, a cathode–anode distance of 4 nm and a bias of 12 V.

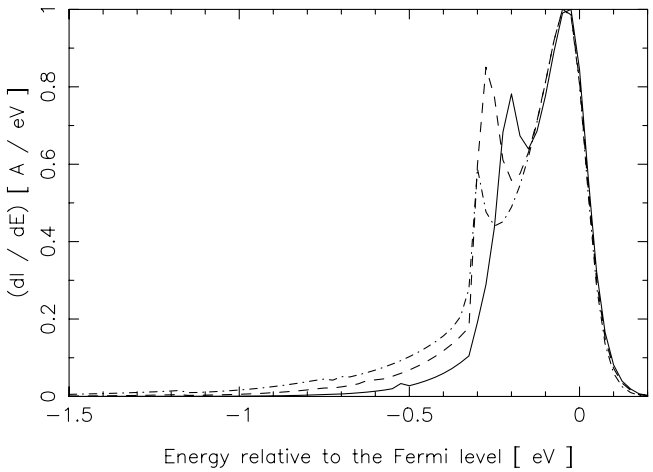

Figure 6. Total-energy distribution of electrons field-emitted from half of a C_{60} molecule on top of a metallic cylinder, for applied electric fields of 2 (solid), 2.5 (dashed) and 3 (dot–dashed) V nm^{-1}. The maxima of the three distributions are respectively 0.104×10^{-11}, 0.340×10^{-9} and 0.147×10^{-7} A eV^{-1}.

The shape and amplitude of the distributions are enlarged as expected since the aspect ratio of the emitter is increased. The bump mentioned in the previous simulation is this time clearly visible, for the three values of the electric field. The peak moves to lower energies as the field increases. These peak displacements are commonly observed and attributed to field penetration at the apex of the emitter [3, 14].

The current extracted for the three values of the electric field is respectively 0.28×10^{-12}, 0.11×10^{-9} and 0.45×10^{-8} A. On average the current extracted from this structure is multiplied by seven orders of magnitude (compared to the situation where the half C_{60} molecule stands on the flat metal). For the 2.5 V nm^{-1} extraction field, the current is multiplied by a factor of 3×10^7. The field enhancement factor derived from the Fowler–Nordheim representation of our data is 3.6 (the alignment of the data obtained with this structure and those considered

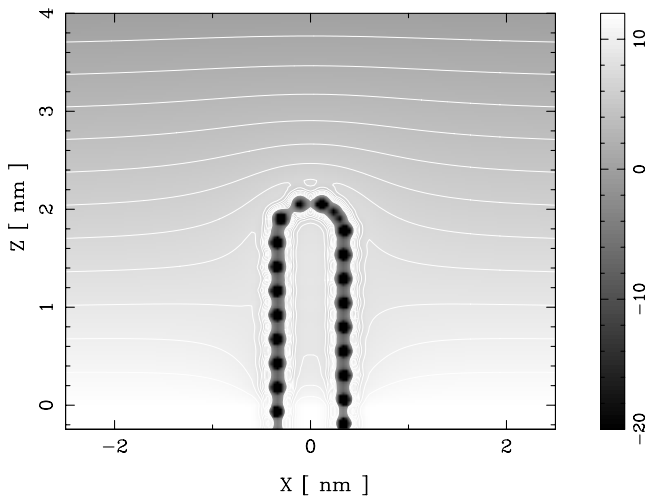

Figure 7. Potential-energy distribution (section in the xz-plane) corresponding to a closed (5, 5) nanotube, a cathode–anode distance of 4 nm and a bias of 12 V. The region below $z = 0$ is repeated 16 times in order to reproduce appropriate band-structure effects.

hereafter is however not as good as for the two previous ones). This number roughly agrees with the aspect ratio of the structure. The field enhancement factors found for the half C_{60} on the flat surface or on top of the metallic cylinder are consistent with the corresponding threshold fields, in the sense that the product between the field enhancement factor and the threshold field gives approximately the same result in both situations.

3.4. Field emission from a closed (5, 5) nanotube

The structure considered in the following simulation is the closed (5, 5) nanotube. Seven basic units of this structure are included in region II containing the fields, so the dimensions of the nanotube body match those of the cylinder considered previously, considering the width of the atomic potentials (the length and radius of these basic units are respectively 0.246 and 0.339 nm). The cap of the nanotube is the half C_{60} molecule of the two previous simulations. In order to reproduce band-structure effects in the energy distributions, 16 additional units of the nanotube are included in an intermediate region between the metallic substrate and region II. Since we artificially enforce this intermediate region to be field free, it does not affect the potential energy in region II. The potential-energy distribution corresponding to an extraction field of 3 V nm^{-1} is illustrated in figure 7. The total-energy distributions corresponding to applied electric fields of 2, 2.5 and 3 V nm^{-1} are represented in figure 8.

The details of the distributions presented in figure 8 have been discussed elsewhere [28]. The peaks in the distributions come from stationary waves in the structure, except for the peak at 0.3 eV below the Fermi level (for the 3 V nm^{-1} electric field). This last peak is that observed in the previous simulations, where a half C_{60} molecule was involved. This observation proves its origin in a (quasi-)localized state at the apex of the closed (5, 5) nanotube. The peak displacements are again a consequence of field penetration in the structure, which lowers the potential energy at the apex of the structure as well as its mean value in the whole structure. The energy distributions are wider than those obtained with the half C_{60} molecule because of the thinner surface barrier.

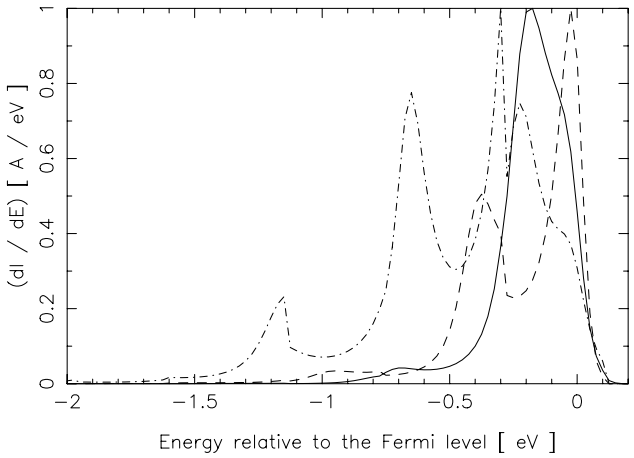

Figure 8. Total-energy distribution of electrons field-emitted from a closed (5, 5) nanotube, for applied electric fields of 2 (solid), 2.5 (dashed) and 3 (dot–dashed) V nm^{-1}. The maxima of the three distributions are respectively 0.566×10^{-11}, 0.270×10^{-8} and 0.389×10^{-7} A eV^{-1}.

The existence of localized states at the cap of closed (5, 5) nanotubes is reported in [15, 19]. The fact they are manifested as resonances in the energy distribution of the emitted electrons (instead of antiresonances) is a consequence of the applied electric field, which introduces a coupling between the cap's localized states and states in the continuous part of the tube's energy spectrum (transforming the localized states into quasi-localized ones). Transition resonances associated with (quasi-)localized states at the apex of closed nanotubes were observed by scanning tunnelling microscopy in [16, 18]. Sharp peaks associated with (quasi-)localized states were also observed in field-emission spectra, both experimentally [2, 3, 14] and theoretically (in the study of open (10, 0) tubes) [13].

The current extracted for the three values of the electric field is respectively 0.16×10^{-11}, 0.72×10^{-9} and 0.18×10^{-7} A. On average the current extracted from this structure is multiplied by a factor of five compared to the half C_{60} standing on a metallic cylinder. The reason comes from the surface barrier, which is lower because the body of the nanotube is not at a rigorously constant potential (unlike the metallic cylinder). The field enhancement factor derived from the Fowler–Nordheim representation of our data is 3.7. This number is quite close to the 3.6 value found for the previous structure whose aspect ratio is identical.

3.5. Field emission from open (5, 5) nanotubes

The previously capped (5, 5) nanotube can be made open by removing the half C_{60} molecule standing on top of it. The ideally open (5, 5) structure obtained in this way is not expected to be stable (see [36, 37]), because its dangling bonds are likely to lead to a reconstruction of the apex of the tube or bind chemically with gaseous species (the case of a saturation by hydrogen is discussed hereafter). For the purpose of comparison with results obtained with a closed (5, 5) nanotube, it is however interesting to study the field-emission properties of these ideally open structures (this was done in detail in [28]).

The potential-energy distribution corresponding to an extraction field of 3 V nm^{-1} is illustrated in figure 9. One can observe that removing the cap leads to a higher field penetration in the structure. The total-energy distributions corresponding to applied electric fields of 2, 2.5 and 3 V nm^{-1} are represented in figure 10. The peaks in this figure are similar to those of figure 8, which was associated with the capped (5, 5) nanotube. The peaks that come from

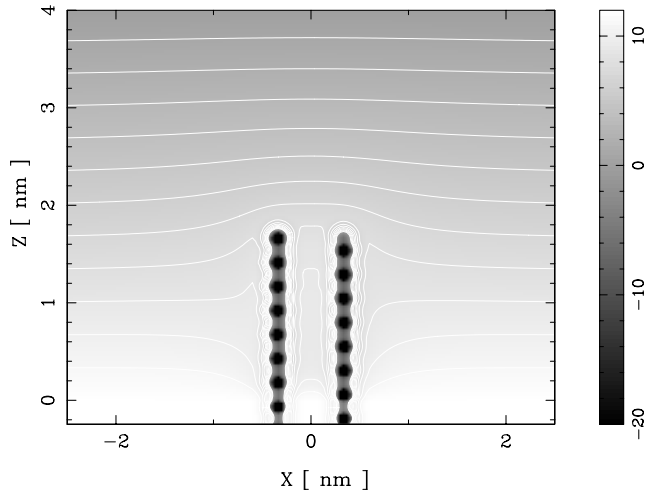

Figure 9. Potential-energy distribution (section in the xz-plane) corresponding to an ideally open (5, 5) nanotube, a cathode–anode distance of 4 nm and a bias of 12 V. The region below $z = 0$ is repeated 16 times in order to reproduce appropriate band-structure effects.

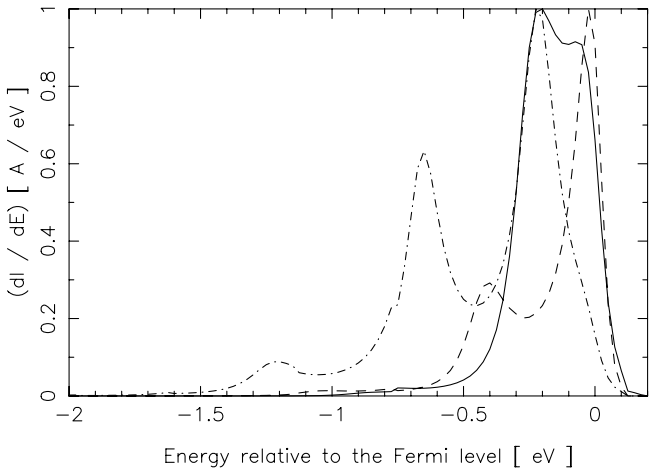

Figure 10. Total-energy distribution of electrons field-emitted from an ideally open (5, 5) nanotube, for applied electric fields of 2 (solid), 2.5 (dashed) and 3 (dot–dashed) V nm^{-1}. The maxima of the three distributions are respectively 0.114×10^{-9}, 0.866×10^{-7} and 0.814×10^{-6} A eV^{-1}.

stationary waves in the cylindrical part of the nanotube are essentially the same, while the peak associated with the cap's quasi-localized state has disappeared. In all cases the contribution to $\mathrm{d}I/\mathrm{d}E$ at the Fermi level is more pronounced, because of the higher transmission probability associated with the increased field penetration. The fact that open (5, 5) nanotubes have high emission rates at the Fermi level (where the electron supply from the metallic substrate is the highest) was also observed by Adessi and Devel [13].

The current extracted for the three values of the electric field is respectively 0.38×10^{-10}, 0.20×10^{-7} and 0.34×10^{-6} A. On average the current extracted from this structure is multiplied by a factor of 20, compared to the case where the nanotube is closed. This enhanced emission

is essentially a consequence of the higher field penetration in the structure (which lowers the surface barrier). Other factors, including an increased emission area and the rounded edges of the open structure, also contribute to this current enhancement. The field enhancement factor derived from the Fowler–Nordheim representation of this data is 3.8, which is comparable with the 3.7 value obtained with the closed (5, 5) (despite the different geometrical aspect ratios).

The open (5, 5) nanotube can be made structurally stable by saturating its dangling bonds with hydrogen. As explained in [26] and observed experimentally [38], this operation results in high magnifications of the emission (up to factors of 200). This effect can be related to the polarization of the C–H bond, which is oriented in the direction of the field and thus reduces both the height and thickness of the surface barrier (making electronic emission easier). The field-enhancement factor derived from the Fowler–Nordheim representation of our data is 3.4, which is smaller than the previous value of 3.8 (the magnification of the current by two orders of magnitude is not indicated by this factor).

The results presented here agree with *ab initio* calculations of [39] and [20], which confirm that the height of the potential barrier is the lowest for the hydrogen-terminated (5, 5) nanotube while it is the highest for the capped one (the ideally open case staying in between). The results of [39] however indicate that the surface barrier of capped (9, 0) tubes is lower than that of open ones (unlike for (5, 5) nanotubes) and that the highest occupied molecular orbital (HOMO) of capped tubes is higher than that of open ones. This last effect, which is not accounted for by our model, is in favour of an increased emission. It seems however that this effect is not sufficient to contradict our conclusion that capped (5, 5) nanotubes are weaker emitters than their open form, our conclusion being supported by others [13]. In [20] Han and Ihm highlight the role of unpaired dangling bonds, which are expected to enhance the current emission (especially when they are oriented in the direction of the field).

Comparisons between the ideally open (5, 5), (10, 10) and (15, 15) single-wall nanotubes showed that the emission from single-wall nanotubes decreases with increasing radius of the tube [29]. This effect is the consequence of the reduction of the emitter's field enhancement factor. A theoretical study of the dependence of this factor on the tube's dimensions and structure was presented by Adessi and Devel in [40].

3.6. Field emission from an open (5, 5)@(10, 10)@(15, 15) nanotube

The (5, 5)@(10, 10)@(15, 15) multi-wall structure can be obtained from the previous (5, 5) nanotube by considering two additional shells (this situation was analysed in detail in [29]). We have represented in figure 11 the potential-energy distribution obtained with this new structure and an extraction field of 3 V nm^{-1}. The total-energy distributions corresponding to applied electric fields of 2, 2.5 and 3 V nm^{-1} are represented in figure 12.

It can be seen from the equipotentials in figure 11 that there is a deeper penetration of the field in the structure, compared to the single-wall (5, 5) tube. This effect is due to the lower global polarizability of the multi-wall structure, which may come from the fact that the dipoles in neighbouring shells cannot be perfectly aligned (in response to the field) because of their natural tendency to be anti-parallel. As a consequence, the surface barrier is lower and the emission is increased. Indeed, the current extracted for the three values of the electric field is respectively 0.26×10^{-8}, 0.87×10^{-6} and 0.34×10^{-4} A, i.e. around 70 times the values obtained with the ideally open (5, 5) nanotube. The increased number and sharpness of the peaks in figure 12 come from the fact that the multi-wall structure can accommodate more propagating states, which are channelled into a narrower discrete energy range because of the strong interactions between the neighbouring shells. As shown in [29], the current extracted from the (5, 5)@(10, 10)@(15, 15) structure is actually larger than the sum of the

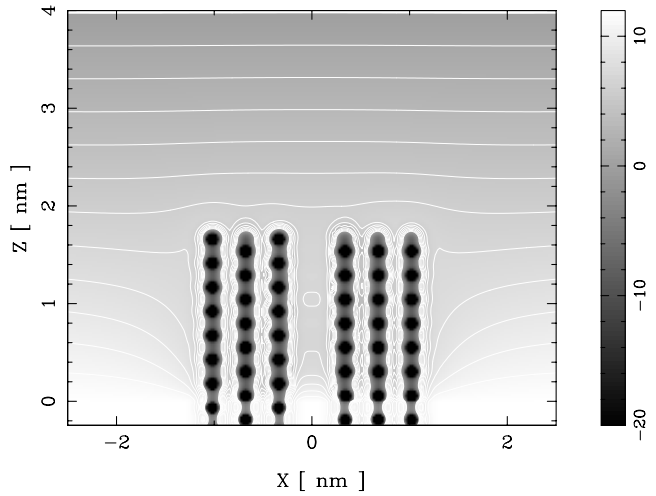

Figure 11. Potential-energy distribution (section in the xz-plane) corresponding to an ideally open (5, 5)@(10, 10)@(15, 15) nanotube, a cathode–anode distance of 4 nm and a bias of 12 V. The region below $z = 0$ is repeated 16 times in order to reproduce appropriate band-structure effects.

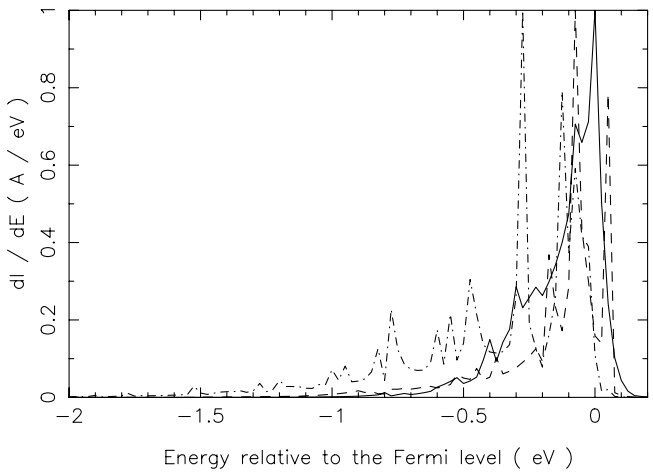

Figure 12. Total-energy distribution of electrons field-emitted from an ideally open (5, 5)@(10, 10)@(15, 15) nanotube, for applied electric fields of 2 (solid), 2.5 (dashed) and 3 (dot–dashed) V nm^{-1}. The maxima of the three distributions are respectively 0.132×10^{-7}, 0.647×10^{-5} and 0.153×10^{-3} A eV^{-1}.

currents extracted from its single-wall components when considered separately. Considering a convex termination, instead of a flat one, results in a deeper penetration of the structure in the potential barrier and leads to a higher emission. The field enhancement factor derived from the Fowler–Nordheim representation of our data is 3.6, which is smaller than the 3.8 value obtained with the ideally open (5, 5) nanotube.

These results are consistent with measurements by Bonard *et al* [2], who showed that closed multi-wall nanotubes are better emitters than both open ones and single-wall tubes. In [20], Han and Ihm point out that multi-wall nanotubes are likely to have unpaired dangling bonds, thus improving their emission properties. In [40], Adessi and Devel show that the field-enhancement factor (as deduced from the direct calculation of the fields) is smaller for

multi-wall nanotubes, compared to single-wall ones. This result does not necessarily contradict our conclusions, since the field values only indicate the slope (at some point) of the potential barrier while our results and argumentation take account of the whole barrier (whose reduced height justifies the higher currents observed here).

4. Discussion

This review of the field-emission properties of carbon protrusions has shown that their emission rate increases with the length of the protrusion (because of the amplification of the field) or because of a higher penetration of the field in the structure. The origins of the increased field penetrations observed in this paper were either structural (removing the cap of single-wall nanotubes), chemical (enforced polarization of C–H bonds) or the reduced polarization capacities of the emitter (due to interactions between the shell of multi-wall nanotubes). Localized states (as observed with the half C_{60}) and unpaired dangling bonds [20] also lead to current enhancements.

The Fowler–Nordheim representation of our data was found to be a straight line for the various protrusions, with a perfect alignment for the isolated carbon atom and the half C_{60} and a small dispersion otherwise. From the slope of this line and within the Fowler–Nordheim theory of field emission, one can derive a 'field enhancement factor', which is actually only an indicator for the degree of variation in the emission as the applied field is changed. It is an effective parameter in the sense that it characterizes a result that actually depends on the details of a three-dimensional barrier (the Fowler–Nordheim theory [11, 12] applies rigorously to flat emitters only).

Although this parameter corresponds roughly to the aspect ratio of the tubes considered, it has no direct interpretation for the first two protrusions considered and does not reflect the various current enhancements (sometimes by orders of magnitude) observed when changing the protrusion. Reaching former conclusions by Cutler *et al* [41], Saenz [42] and Bonard *et al* [43] (who even demonstrated a dependence on the inter-electrode distance), these comparisons thus show that the field enhancement factor, as derived from the Fowler–Nordheim equation, does not reflect the whole physics of the emission process and should certainly not be interpreted literally, especially when dealing with nanometric emitters.

Models like that used here or in [13] and [40] take account of the atomic structure of the nanotubes and solve precisely the scattering through the three-dimensional surface barrier. They deal accurately with the emission part of the problem (outside the nanotube), but only provide a first-order approximation of the electronic processes inside the nanotube.

One issue to consider in order to improve these models and the understanding of experimental results is the electronic configuration of the nanotube. In this context this point is only addressed accurately by *ab initio* techniques [20, 39, 44, 45], at the price of higher computational resources (thus limiting their ability to treat long tubes) and without solving the field-emission part of the problem (see however [46] by Han *et al*). This issue includes the dangling bonds, which were shown in [20] to improve substantially the emission rates. It also addresses the accumulation or transfers of electric charges [39, 44], which affect the potential energy, the local density of states and energy levels at the apex [39, 44, 45] and may induce band-bending effects in the nanotube. Considering dynamic effects (associated with interactions between the emitted electron and those in the tube) may also be of interest. In a more general context, addressing precisely the electronic structure of composite emitters may lead to a better understanding of the triple-junction systems [47] and the ultrathin semiconductor layers [48].

Another issue is the consideration of transport properties [49–53], which include the energy-loss processes that are responsible for resistive effects and heating of the emitter.

Indeed it was shown by Binh *et al* [54] that the temperature of the nanotube can increase up to 2000 K during the emission, making the consideration of these effects necessary at high emission currents.

It is known that adsorbed hydrogen [38], oxygen [55] and water molecules [56] can increase—sometimes by orders of magnitude—the nanotubes' emission rates and that large quantities of these molecules may be stored between the shells of multi-wall structures [57]. Understanding the influence of defects [50–53], substitutional atoms [58] and adsorbed species on the electronic structure of the nanotube, its doping and its transport and field-emission properties is also important.

The last issue we will mention is the back-contact between the nanotube and its usually metallic support [49, 59]. The emission rates can indeed be drastically affected by their distance or the appearance of a Schottky barrier (resulting from the equilibrium of their Fermi levels) [60].

5. Conclusion

This paper is a review presentation of field-emission properties of carbon protrusions, ranging from a single atom to multi-wall nanotubes. The simulations were achieved using a transfer-matrix technique for consideration of three-dimensional aspects of the problem (i.e., the atomic configuration and the surface barrier). Comparing the emission rates of these protrusions enables one to determine how they are affected by the length of the structure, localized states and field penetration (which depends on whether the nanotube is closed or not, on the presence of adsorbed/bonded species and on the polarizability of the structure). We have shown that the field enhancement factor, as deduced from the Fowler–Nordheim representation of our data, does not reflect the whole physics of the emission process and should not be interpreted literally or used as the only factor of consideration when dealing with nanometric emitters. Finally we have indicated some important issues for the understanding and development of field emission from carbon materials.

Acknowledgments

This work was supported by the National Fund for Scientific Research (FNRS) of Belgium and by NSF grant number DMI-0078637 administrated by UHV Technologies, Inc., Mt Laurel, NJ, USA. One of the authors (AM) acknowledges the use of the Namur Scientific Computing Facility and the Belgian State Interuniversity Research Program on 'Quantum size effects in nanostructured materials' (PAI/IUAP P5/01). The authors acknowledge Ph Lambin for useful discussions.

References

[1] de Heer W A, Châtelain A and Ugarte D 1995 *Science* **270** 1179
[2] Bonard J-M, Salvetat J P, Stöckli T, Forró L and Chatelain A 1999 *Appl. Phys.* A **69** 245 and references therein
[3] Fransen M J, van Rooy Th L and Kruit P 1999 *Appl. Surf. Sci.* **146** 312 and references therein
[4] Collins P G and Zettl A 1997 *Phys. Rev.* B **55** 9391
[5] Geis M W, Twichell J C and Lyszczarz T M 1996 *J. Vac. Sci. Technol.* B **14** 2060
[6] Lerner P, Cutler P H and Miskovsky N M 1997 *J. Vac. Sci. Technol.* B **15** 337
[7] Lerner P, Miskovsky N M and Cutler P H 1998 *J. Vac. Sci. Technol.* B **16** 900
[8] Forbes R G 2001 *Solid-State Electron.* **45** 779
[9] Nilsson L, Gröning O, Emmenegger C, Küttel O, Schaller E, Schlapbach L, Kind H, Bonard J-M and Kern K 2000 *Appl. Phys. Lett.* **76** 2071
[10] Filip V, Nicolaescu D, Tanemura M and Okuyama F 2001 *Ultramicroscopy* **79** 39
[11] Fowler R H and Nordheim L 1928 *Proc. R. Soc.* A **119** 173

[12] Good R H and Müller E 1956 *Handbook of Physics* vol 21 (Berlin: Springer) p 176
[13] Adessi Ch and Devel M 2000 *Phys. Rev.* B **62** 13314
[14] Dean K A, Groening O, Küttel O M and Schlapbach L 1999 *Appl. Phys. Lett.* **75** 2773
[15] Tamura R and Tsukada M 1995 *Phys. Rev.* B **52** 6015
[16] Carroll D L, Redlich P, Ajayan P M, Charlier J C, Blase X, De Vita A and Car R 1997 *Phys. Rev. Lett.* **78** 2811
[17] De Vita A, Charlier J C, Blase X and Car R 1999 *Appl. Phys.* A **68** 283
[18] Kim Ph, Odom T W, Huang J L and Lieber C M 1999 *Phys. Rev. Lett.* **82** 1225
[19] Anantram M P and Govindan T R 2000 *Phys. Rev.* B **61** 5020
[20] Han S and Ihm J 2000 *Phys. Rev.* B **61** 9986
[21] Mayer A, Senet P and Vigneron J-P 1999 *J. Phys.: Condens. Matter* **11** 8617
[22] Bachelet G B, Greenside H S, Baraff G A and Schluter M 1981 *Phys. Rev.* B **24** 4745
[23] Mayer A and Vigneron J-P 1997 *Phys. Rev.* B **56** 12599
[24] Mayer A and Vigneron J-P 1988 *J. Phys.: Condens. Matter* **10** 869
Mayer A and Vigneron J-P 1999 *Phys. Rev.* B **60** 2875
Mayer A and Vigneron J-P 1999 *Phys. Rev.* E **59** 4659
Mayer A and Vigneron J-P 2000 *Phys. Rev.* E **61** 5953
[25] Gravil P A, Lambin Ph, Gensterblum G, Henrard L, Senet P and Lucas A A 1995 *Surf. Sci.* **329** 199
[26] Mayer A, Miskovsky N M and Cutler P H 2001 *Appl. Phys. Lett.* **79** 3338
[27] Mayer A, Miskovsky N M and Cutler P H 2002 *J. Vac. Sci. Technol.* B **20** 100
[28] Mayer A, Miskovsky N M and Cutler P H 2002 *Ultramicroscopy* **92** 215
[29] Mayer A, Miskovsky N M and Cutler P H 2002 *Phys. Rev.* B **65** 155420
[30] Mayer A, Miskovsky N M and Cutler P H 2002 *Phys. Rev.* B **65** 195416
[31] Ziman J M 1964 *Principles of the Theory of Solids* (Cambridge: Cambridge University Press) p 46
[32] Liang W, Bockrath M, Bozovic D, Hafner J H, Tinkham M and Park H 2001 *Nature* **411** 665
[33] Dresselhaus M S, Dresselhaus G, Eklund P C and Saito R 2000 *Optical and Electronic Properties of Fullerenes and Fullerene-Based Materials* (New York: Dekker) p 236
[34] Lang N D, Yacoby A and Imry Y 1989 *Phys. Rev. Lett.* **63** 1499
[35] Lucas A A, Morawitz H, Henry G R, Vigneron J-P, Lambin Ph, Cutler P H and Feuchtwang T E 1988 *Phys. Rev.* B **37** 10708
[36] Lou L, Nordlander P and Smalley R E 1995 *Phys. Rev.* B **52** 1429
[37] Charlier J, De Vita A, Blase X and Car R 1997 *Science* **275** 646
[38] Shaw J 2001 Naval Research Laboratory, private communication
[39] Luo J, Peng L-M, Xue Z Q and Wu J L 2002 *Phys. Rev.* B **66** 155407
[40] Adessi Ch and Devel M 2002 *Phys. Rev.* B **65** 075418
[41] Cutler P H, He J, Miskovsky N M, Sullivan T E and Weiss B 1993 *J. Vac. Sci. Technol.* B **11** 387
[42] Saenz J J 2001 *3rd Eur. Field Emission Workshop (Alicante, Spain)* (oral presentation)
[43] Bonard J-M, Croci M, Arfaoui I, Noury O, Sarangi D and Châtelain A 2002 *Diamond Relat. Mater.* **11** 763
[44] Kim C, Kim B, Lee S M, Jo C and Lee Y H 2002 *Phys. Rev.* B **65** 165418
[45] Zhou G, Duan W and Gu B 2001 *Phys. Rev. Lett.* **87** 095504
[46] Han S, Lee M H and Ihm J 2002 *Phys. Rev.* B **65** 085405
[47] Geis M W, Efremow N N, Krohn K E, Twichell J C, Lyszczarz T M, Kalish R, Greer J A and Tabat M D 1997 *Linc. Lab. J.* **10** 3
[48] Binh V T and Adessi Ch 2000 *Phys. Rev. Lett.* **85** 864
[49] Krompiewski S, Martinek J and Barnás J 2002 *Phys. Rev.* B **66** 073412
[50] Chico L, Benedict L X, Louie S G and Cohen M L 1996 *Phys. Rev.* B **54** 2600
[51] Choi H J and Ihm J 1999 *Solid State Commun.* **111** 385
[52] Choi H J, Ihm J, Louie S G and Cohen M L 2000 *Phys. Rev. Lett.* **84** 2917
[53] Roche S and Saito R 1999 *Phys. Rev.* B **59** 5242
[54] Purcell S T, Vincent P, Journet C and Binh V T 2002 *Phys. Rev. Lett.* **88** 105502
[55] Park N, Han S and Ihm J 2001 *Phys. Rev.* B **64** 125401
[56] Maiti A, Andzelm J, Tanpipat N and von Allmen P 2001 *Phys. Rev. Lett.* **87** 155502
[57] Nishikawa O, Murakami T, Watanabe M, Yagyu T and Taniguchi M 2002 *Proc. 201st Mtg of the Electrochemical Society 2002-1* (Princeton, NJ: Electrochemical Society) p 444
[58] Zhang G, Duan W and Gu B 2002 *Appl. Phys. Rev.* **80** 2589
[59] Anantram M P, Datta S and Xue Y 2000 *Phys. Rev.* B **61** 14219
[60] Heinze S, Tersoff J, Martel R, Derycke V, Appenzeller J and Avouris Ph 2002 *Phys. Rev. Lett.* **89** 106801